Available online at www.sciencedirect.com
SCIENCE DIRECT®
Journal of Nuclear Materials 323 (2003) 1–7
journal of nuclear materials
www.elsevier.com/locate/jnucmat

Characterisation of secondary products of uranium–aluminium material test reactor fuel element corrosion in repository-relevant brine

L. Mazeina [1], H. Curtius *, J. Fachinger, R. Odoj

Institute for Safety Research and Reactor Technology, Forschungszentrum Jülich, 52425 Jülich, Germany

Received 7 March 2003; accepted 16 June 2003

Abstract

Corrosion experiments with non-irradiated uranium–aluminium fuel elements were performed in $MgCl_2$-rich brine. Distribution analysis of corroded material showed that about 90% of the initially available metallic U and Al precipitated. Investigations of these secondary corrosion products provided that one component is a Mg–Al–Cl–hydrotalcite.

1. Introduction

The final disposal of spent fuel elements from research reactors in deep geological formations is under discussion as a national waste management option in Germany. The main requirement for final disposal is reliable and safe storage of the radioactive waste for a long time. In long-term safety analysis possible accident scenarios also have to be taken into account. In Germany, the Gorleben salt dome is under consideration as a final repository for highly active waste, including Material Test Reactor Fuel Elements (MTR-FE) from the research reactor DIDO, Jülich. The material for research reactor fuel elements are completely different from fuel elements of nuclear power plants for electricity production. As fuel, MTR-FE have a metallic uranium–aluminium alloy covered with Al [1]. The spent fuel elements will be placed in a cast-iron container (POLLUX) for final disposal. An accident scenario for a salt dome, which cannot be ruled out totally for a time period of hundred thousand years, is a water ingress which creates highly concentrated salt brines. Previous investigations showed that the MTR-FE are not stable in these salt brines; corrosion occurs and radionuclides are released [1]. The distribution of the released radionuclides between the newly formed solid corrosion products and the solution showed that about 90% of the radionuclides are immobilised by the corrosion products (secondary phases) [1]. Due to the high dose rate of irradiated fuel it was not possible to determine the structures, chemical speciations and compositions of the solid corrosion products.

The identification of the secondary phases is essential because these phases may control the concentration of dissolved radionuclides in the leaching solution [2], for example, by immobilisation. Since irradiated uranium–aluminium MTR-FE have practically the same chemical uranium–aluminium matrix as non-irradiated MTR-FE [3], we assume that non-irradiated uranium–aluminium MTR-FE will have a nearly identical corrosion behaviour leading to almost identical main secondary phases. Therefore, corrosion experiments with non-irradiated MTR-FE have been performed to clarify the nature, chemical composition and structure of the corrosion products.

* Corresponding author. Tel.: +49-2461 61 4205; fax: +49-2461 61 2992.
E-mail address: h.curtius@fz-juelich.de (H. Curtius).
[1] Present address: Thermochemistry Facility, University of California at Davis, One Shields Avenue, Davis, CA 95616, USA.

0022-3115/$ - see front matter © 2003 Published by Elsevier B.V.
doi:10.1016/S0022-3115(03)00316-7

2. Experimental

The corrosion experiments were performed in three glass autoclaves at 90 °C under initial Ar atmosphere using $MgCl_2$-rich brine (relevant for Gorleben salt dome). Fe^0 was added to simulate the presence of the iron system due to the corrosion of the cast-iron container. To investigate the corrosion at different surface-to-volume ratios three experiments were performed: two with one and one with four non-irradiated MTR-FE plates in the same volume. The details of the experiments are summarised in Table 1.

Uranium–aluminium plates used were cut from a non-irradiated fuel element of the material test reactor DIDO, Jülich, Germany. The size of uranium–aluminium plate pieces used is $20 \times 28 \times 1.5$ mm^3 with a mass of about 1.9 g. The uranium content in the piece is about 0.087 g (4.5 wt%). Fe^0 was added as cast-iron plate, GGG40, with the composition Fe (93%), C (3.45–3.8%), Si (2.6–2.9%), Mn (0.25–0.50%), S (0.005–0.01%). The average was 3.3 g.

$MgCl_2$ brine, representing one of the repository-relevant solutions for the Gorleben salt dome, has the following composition: 937.1 g/l $MgCl_2 \cdot 6H_2O$, 39.68 g/l $CaCl_2 \cdot 2H_2O$, 4.13 g/l NaCl, 1.42 g/l KCl and 0.126 g/l $MgSO_4 \cdot 7H_2O$ (see chemical composition in [4]). All chemicals were from Merck, Darmstadt, and of analytical grade. The salts were dissolved in deionised water at 70 °C. Heating was stopped when the solution became clear. After cooling the solution was placed in a volumetric flask.

Before starting the experiments, Ar first was bubbled through the solution to remove dissolved gases (CO_2, O_2 etc.). Then the plates were added in such way that they did not come into contact with each other. The closed autoclaves were placed in a Heraeus desiccator at 90 °C.

At different time intervals the autoclaves were opened under an Ar atmosphere to take solution samples. The samples were filtered (450 nm filter) and the pH was measured immediately under an Ar atmosphere at 90 °C. The measurements were performed with a pH-meter Metrohm, Filderstadt, type 691, using a combination ROSS pH-electrode Orion Co., type 8130, calibrated with Merck buffer solutions. All pH values measured were corrected for highly concentrated brines according to [4]. Solution samples were then diluted (1 ml of sample with 9 ml 0.1 M HNO_3) and analysed by ICP-OES (type 3520 B, ARL Instruments, Ecublens, Switzerland). Chloride was determined by a spectral photometer CADAS 100, Dr. Lange, with Dr. Lange cuvette chloride tests LCK 311.

After the experiments the autoclaves were opened and the liquid and solid phases were separated and stored in Ar atmosphere. Aliquots of the sediment phases were treated in different ways: one wet aliquot was dried at 90 °C for about 24 h and another aliquot was dialysed. For the dialysis, a dialysis hose VISKING, type 36/32, was filled with the substance (2–4 g) and placed in a 2 l vessel containing deionised water. The water was changed twice a day for 2–5 days. After dialysis, the substance was dried at 90 °C for 24 h. Samples of sludge were scrapped off the surface of not completely corroded plates, then treated the same way as described above. All dried samples were milled to powder and then analysed by XRD (Stoe Stadi transmission diffractometer coupled to a Co anode X-ray tube and using CoKα radiation with $\lambda = 178.8970$ pm at 40 kV and 30 mA) and SEM (Jeol JSM 840). To analyse the elemental composition of the solid an aliquot of 0.2 g was dissolved with 5 ml 8 M HNO_3. The clear solution obtained was analysed by ICP-OES; the chloride concentration was measured photometrically. The uranium activity was analysed by α-spectrometry (α-analyser, Canberra-Packard GmbH). For these purposes, U was extracted from the liquid samples with TOPO (tetraoctylphosphinoxide). From the specific activity the masses of different U isotopes were calculated and summarised.

Table 1
Experimental details of the corrosion experiments in the autoclaves

	Autoclave		
	1	2	3
Solution	$MgCl_2$ brine	$MgCl_2$ brine	$MgCl_2$ brine
Volume of solution, ml	400	400	400
Number of MTR-FE plates	1	1	4
Weight of MTR-FE plates	1.84	2.03	7.91
Iron speciation	GGG40	–	GGG40
Weight of iron, g	2.99	–	2.96
Temperature, °C	90	90	90
Environment	Ar	Ar	Ar
Duration of the experiment, days	525	605	157

3. Results and discussion

The two experiments with one plate of non-irradiated uranium–aluminium fuel element (autoclave 1 with iron and autoclave 2 without iron) were finished after the plates corroded totally and no further pressure increase was observed. In both experiments the complete corrosion of the plates lasted the same time. The experiment with four plates (autoclave 3 with iron) was stopped before they corroded completely. Observable changes in incompletely corroded plates from autoclave 3 are shown in Fig. 1. The layer of secondary phases on the surface can be seen very distinctly.

Significant amounts of corrosion products (secondary phases) were formed in all experiments. Visually, the secondary phases appear as a coarse-grained material in the lower part and small-grained material in the upper part. In all experiments the sediments were white with green-coloured areas (probably UO_2).

The element compositions of the solid phases are given in Table 2. The main elements of the secondary phases are Mg and Al. The large amount of Mg in the sediment is due to the oversaturation of $MgCl_2 \cdot 6H_2O$. From analytical data it can be seen that all initially available metallic aluminium corroded and metallic uranium precipitated (Table 3). After dialysis the sediments are enriched by Al and U, that means that Al and U are components of insoluble phases.

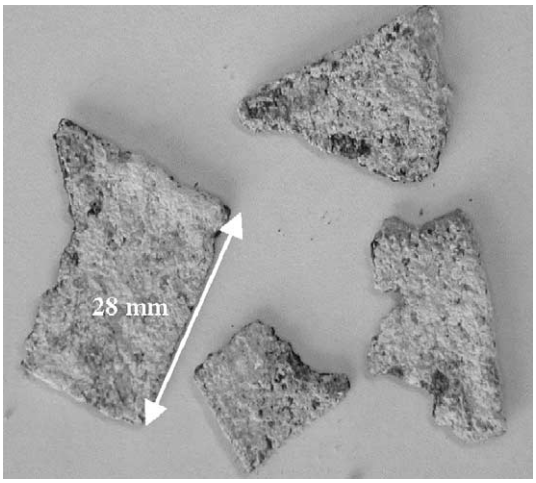

Fig. 1. Plates of non-irradiated material test reactor fuel elements after 160 days of leaching in $MgCl_2$-rich brine at 90 °C (autodalve 3).

XRD analysis showed that the solid phases are divided into amorphous and crystalline parts. The crystalline part is represented by $MgCl_2 \cdot 6H_2O$ and by a phase with the structure of a hydrotalcite-like compounds. In autoclaves 1 and 3, hydrotalcite-like compound peaks were already found in untreated (undialysed) substance (see Figs. 2–4). The XRD

Table 2
Element composition and amount of corrosion products, wt%[a]

Autoclave	Amount of sediment, g	Mg	Al	U	After dialysis	
					U	Al
1	30	11	4.5	0.37	n.m.	20
2	20	11	5.9	0.70	5.3	31
3	100	9.5	7.1	0.64	0.64	18

[a] The rest is water, chloride and minor elements (less than 2%).

Table 3
Aluminium and uranium distribution between solid and liquid phases after experiments were finished

Autoclave	Initially		Remained uncorroded		In solution		In sediment	
	g	%	g	%	g	%	g	%
Aluminium distribution								
1[a]	1.60 ± 0.13	100	0	0	0.008	<1	1.4	84
2[a]	1.77 ± 0.14	100	0	0	0.024	1.4	1.2	67
3[a]	6.88 ± 0.55	100	1.1 ± 0.15	16	0.019	<1	6.4	93
Uranium distribution								
1[a]	140 ± 30	100	0	0	2.8	2	120	86
2[a]	150 ± 30	100	0	0	4.2	2.8	140	93
3[a]	590 ± 120	100	54 ± 5	9	3.7	<1	580	98

[a] The derivation of total sum from 100% is due to the experimental error.

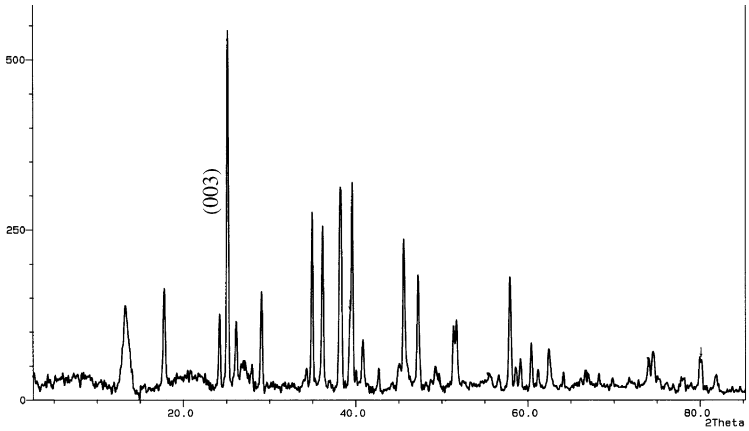

(a) untreated sample

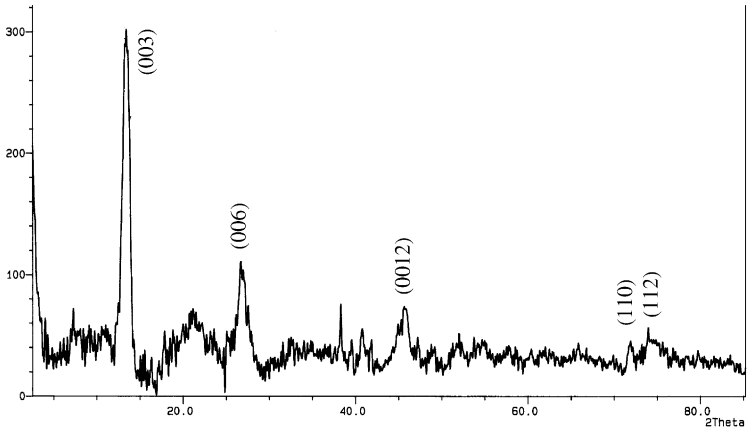

(b) dialysed sample

Fig. 2. XRD pattern of the sediment from autoclave 1 (not-indicated peaks belong to bishofite).

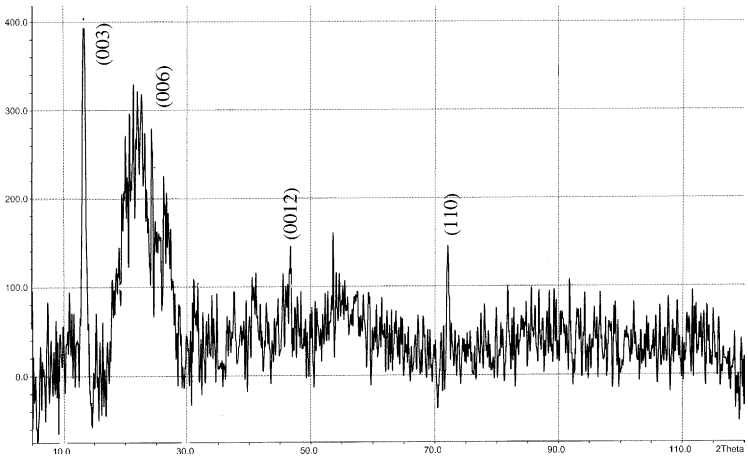

Fig. 3. XRD pattern of dialysed substance from autoclave 2.

patterns of dialysed samples from autoclaves 2 and 3 also showed amorphous admixtures. Nevertheless, in all autoclaves the hydrotalcite peaks (especially the peak with $hkl = 003$) were identified. The highest concentra-

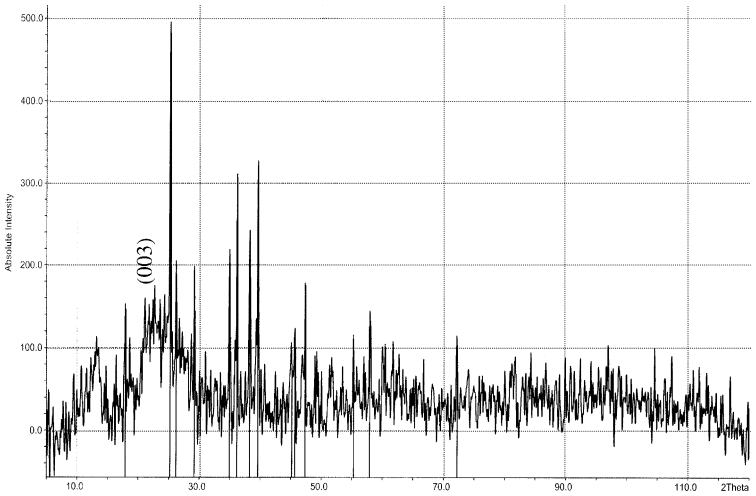

(a) untreated sample

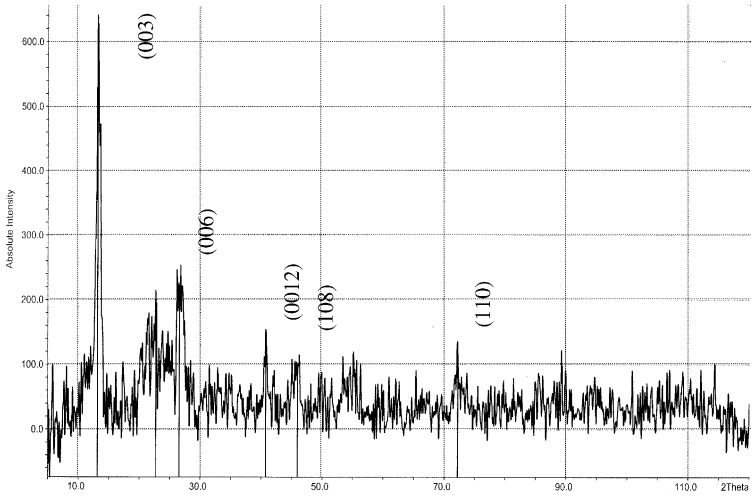

(b) dialysed sample

Fig. 4. XRD pattern of the sediment from autoclave 3 (not-indicated peaks belong to bishofite).

tion of hydrotalcite was found in the glass holder in which the plates were placed and on the surface of an incompletely corroded plate from autoclave 3. An explanation for this observation is given later.

The lattice parameters *a* and *c* were calculated from the XRD data (Table 4). The hydrotalcites found in the secondary phase belong to Cl-HTlc with a Mg/Al ratio close to 2. A Mg/Al ratio of 3 was found only in experiment 1. Nevertheless, the analytically determined ratio of Mg/Al for hydrotalcites from autoclaves 2 and 3 is lower because of the presence of amorphous phases.

The morphology of the Mg–Al–HTlcs obtained was investigated by SEM. The highest concentration of hydrotalcite crystals appeared on the metallic surface. The sand rose crystal structure, typical of hydrotalcites, can be clearly seen. The same structure was identified by previous researchers [2,5,6]. The hydrotalcite-like compound crystals from autoclave 1 and 3 have different sizes: about 2 μm from autoclave 1 and about 0.5 μm

Table 4
Lattice parameters and element ratio for the hydrotalcites obtained

Autoclave	c (d_{003}), pm	a (d_{110}), pm	Mg/Al[a]	Al/Cl[a]
1	2328	305.3	2.8	2.1
2	2306	304.0	1.4	–
3	2337	303.6	0.5	2.1

[a] Calculated from analytically determined values.

from autoclave 3. The reason for these differences is that the crystal size increased with time of alteration [2] (525 days for autoclave 1 and 157 days for autoclave 3) due to the presence of a large amount of amorphous phases (Fig. 5).

No sharp SEM micrograph was obtained for the sediment of autoclave 2.

The HTlcs were found by Abdelous et al. [2] as an alteration product of nuclear waste glass and basaltic glass in $MgCl_2$-rich brine. It is therefore interesting to note that the corrosion of nuclear waste glass, basaltic glass [2], corrosion of metallic Al [7] and uranium–aluminium fuel elements (this work) in $MgCl_2$-rich brine led to the formation of hydrotalcite.

As reported for hydrotalcite synthesis, formation of hydrotalcite normally happens at pH = 8–10 [8]. Final pH values for experiments 1 and 2 were 3.8, and for experiment 3 about 2.3. That means that the highest pH value in the bulk solution for hydrotalcite formation was not higher than 3.8 (corrected value about 5.7). The reason is that formation of hydrotalcite during the corrosion experiments at lower pH must happen in a different manner than the formation of hydrotalcite through synthesis. Hydrotalcite is formed by synthesis as a co-precipitation of $Mg(OH)_2$ and $Al(OH)_3$ in the bulk solution. The formation of hydrotalcite is also due to co-precipitation during the corrosion experiments. However, it takes place in the pits, not in the bulk solution. The proposed mechanism can be described as follows.

Highly concentrated chloride medium causes a very fast destruction of the Al oxide surface film and the formation of pits on the metallic surface. Aluminium ions are released from these pits

$$Al^0 \Longleftrightarrow Al^{3+} + 3e^- \quad E_0 = -1.667\ V \tag{1}$$

Moreover, an Al hydrolysis occurs in the pits leading finally to the precipitation of $Al(OH)_3$ as summarised:

$$Al^{3+} + 3H_2O \Longleftrightarrow Al(OH)_3 \downarrow + 3H^+ \tag{2}$$

Protons are produced by hydrolysis and diffuse inside the pits and are then reduced to H_2 [9]. Due to the hydrogen reduction the pH increases and $Mg(OH)_2$ may precipitate. The precipitation of $Mg(OH)_2$ and $Al(OH)_3$ could happen separately in a locally close area, but Mg–Al–hydrotalcite formation by co-precipitation of these hydroxides is more favoured. The surface of the plate plays a catalytic role in hydrotalcite formation. An experimental proof of this was given by the fact that most of the hydrotalcite was found in the glass holder and some on the surface of incompletely corroded plates.

Hydrotalcite-like compounds are a large family of double-layer hydroxides with a big variety of metals and anions [8,10]. Hydroxide layers are positively charged and deposited on each other and different anions occur in the interlayer space to balance the positive charge. The variety of anions is enormous including those formed by radioactive elements [11–14]. The interlayer anions can be quite easily replaced by anions present in the surrounding aquatic medium [15], therefore another name for hydrotalcite-like compounds is anionic clays. Most geological materials (cationic clays and zeolites, for example) are suitable for cation sorption, therefore the ability of hydrotalcite-like compounds to exchange radioactive anions, e.g. iodide, makes hydrotalcites attractive for the immobilisation of radioactive anions. Moreover, there is also a possibility of cation sorption because the OH^- groups on the surface can act as proton acceptors [16]. The formation of hydrotalcite as a corrosion secondary product in repository-relevant brine and their properties with respect to radionuclide retardation make hydrotalcites even attractive as backfill material in a final repository.

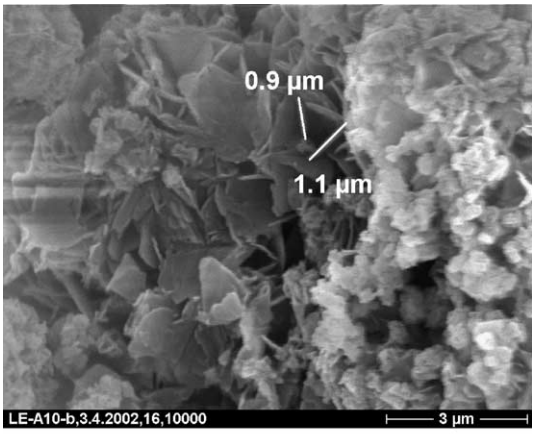

autoclave 1 (magnification 10000 times)

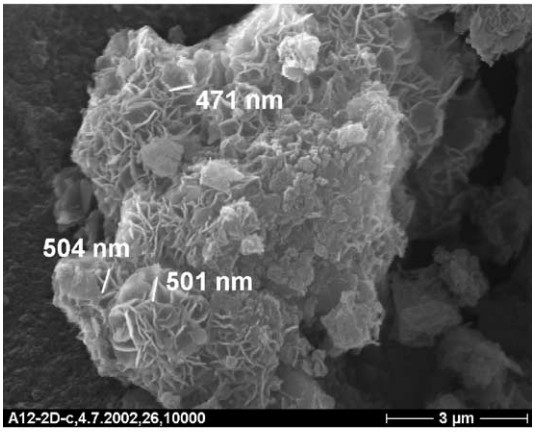

autoclave 3 (magnification 10000 times)

Fig. 5. SEM micrographs of hydrotalcites from corrosion experiments.

4. Conclusions

Significant amounts of corrosion products were formed in leaching experiments with the plates of non-irradiated uranium–aluminium material test reactor fuel element (MTR-FE) plates in $MgCl_2$-rich brine. The main elements of the secondary phases are Mg and Al. Uranium is a minor component. Analysis showed that nearly the greatest part of dissolved Al and U precipitated in the secondary phases. This fact is important for the final disposal strategy: even in the case of an accidental scenario (water ingress in the Gorleben salt dome) and complete corrosion of irradiated fuel elements, the dissolved material will precipitate, which is especially important for predicting uranium mobility.

The corrosion products of uranium–aluminium fuel elements consisted of an amorphous and a crystalline part. Bischofite and Mg–Al–Cl-hydrotalcite were identified in the crystalline part. The latter compound was identified for the first time in corrosion experiments with non-irradiated uranium–aluminium MTR-FE. The formation of these hydrotalcites under the given conditions was possible because of the available metallic aluminium surface and highly aggressive chloride medium ($MgCl_2$-rich brine). The intensive pitting corrosion creates local areas of different pH values, consequently brucite ($Mg(OH)_2$) and gibbsite ($Al(OH)_3$) can be co-precipitated and form the hydrotalcite.

Taking into account that an irradiated MTR-FE has the same uranium–aluminium metallic matrix as non-irradiated MTR-FE, identical secondary phases, containing hydrotalcites can be expected in the case of an accident scenario during the final storage in a salt dome. The retardation of released radionuclides of an irradiated MTR-FE by secondary phases as described in [1] can be now partly explained through the presence of hydrotalcites. Nevertheless, dealing with irradiated fuel elements the behaviour of the decay elements must be investigated in future.

References

[1] H. Brücher, H. Curtius, J. Fachinger, Transactions 5th Topical Meeting on Research Reactor Fuel Management, 2001, Aachen, Germany, ENS RRFM.
[2] A. Abdelouas, J.L. Crovisier, W. Lutze, B. Fritz, A. Mosser, R. Müller, Clays Clay Miner. 42 (1994) 526.
[3] J. Fachinger, H. Brücher, K. Nau, G. Kaiser, H. Rainer, Syuhada, S. Zschunke, Untersuchungen zur Radionuklidfreisetzung durch Einwirkung konzentrierter Salzlaugen auf Alu-MTR-Brennelemente, Berichte des Forschungszentrums Jülich, Jül-3694, 1998.
[4] B. Grambow, R. Müller, Material Resources Society Symposium Proceedings, vol. 176, 1990.
[5] C. Mistra, J. Perrota, Clays Clay Miner. 40 (1992) 145.
[6] U. Olsbye, D. Akporiaye, E. Rytter, M. Rønnekleiv, E. Tangstad, Appl. Catal. 224 (2002) 39.
[7] L. Mazeina, H. Curtius, J. Fachinger, Clay Miner. 38 (2003) 35.
[8] F. Cavani, F. Trifiro, A. Vaccari, Catal. Today 11 (1991) 173.
[9] H.P. Godard, W.B. Jepson, M.R. Bothwell, R.L. Kane, The Corrosion of Light Metals, John Wiley, 1967.
[10] S. Miyata, Clays Clay Miner. 23 (1975) 369.
[11] K. Chibwe, W.J. Jones, Chem. Soc. Chem. Commun. (1989) 926.
[12] J.M. Fernandez, C. Barriga, M.A. Ulibarri, F.M. Labajos, V. Rives, Chem. Mater. 9 (1997) 312.
[13] G. Fetter, E. Ramos, M.T. Olguin, P. Bosch, T. Lopez, S.J. Bulbulian, Radioanal. Nucl. Chem. 221 (1997) 63.
[14] M.A. Ulibarri, I. Pavlovic, C. Barriga, M.C. Hermosín, J. Cornejo, Appl. Clay Sci. 18 (2001) 17.
[15] S. Miyata, Clays Clay Miner. 31 (1983) 305.
[16] M. Lehmann, A.I. Zouboulis, K.A. Matis, Chemosphere 39 (1999) 881.